

DEVELOPMENT OF A SHAPE MEMORY ALLOY WIRE ACTUATOR TO OPERATE A MORPHING WING

MISUN RIM

KAIST, School of Mechanical, Aerospace and Systems Engineering, Daejeon, Korea

EUN-HO KIM

University of South Carolina, Department of Mechanical Engineering, Columbia, USA

WOO-RAM KANG, IN LEE

KAIST, School of Mechanical, Aerospace and Systems Engineering, Daejeon, Korea

e-mail: inlee@kaist.ac.kr

DSC tests were performed on several types of SMAs to verify the phase-transformation temperatures, and then experiments to examine their characteristics were carried out. An electric-current was supplied to the SMA wire to measure the appropriate operational current range. The force generated by the SMA wire increased according to the supplied current, but it diminished when the over-current was supplied because thermo-mechanical properties of the wire started to degrade. The appropriate stress range for effective actuation characteristics was also investigated. The SMA wire actuator was designed to operate a morphing wing. Experiments for the wing were conducted to verify its characteristics and it was smoothly deformed.

Keywords: morphing wing, shape memory alloy (SMA), wire actuator

1. Introduction

Aircraft characteristics should be optimized according to purposes and flight conditions (Joshi *et al.*, 2004; Bowman *et al.*, 2007). Commercial passenger aircrafts are designed for a long distance cruising, whereas combat aircrafts are designed for a short distance and a fast operation (Sanders *et al.*, 2003, 2005). Recent aerodynamic research has focused on active working systems which are called smart structures for a variety of purposes or a need. A morphing wing is one type of smart structures. Morphing can be classified in terms of two purposes. One is “configuration morphing”, which entails changes in the span and the sweepback angle (Diaconu *et al.*, 2008; Mattioni *et al.*, 2006). This morphing can lead to multi-mission capabilities and improved mobility difficult to achieve with a conventional fixed wing. The other one is “maneuver morphing”, which creates a controllable winglet to minimize vortices at the blade tip and vortices induced by flap changes. This morphing can improve aerodynamic efficiency during operation by replacing the parts that cause aerodynamic losses.

Most aircrafts use high-lift systems, which are connected by hinges, and they are passively operated by more than one hydraulic actuator. For high aircraft efficiency, gaps between parts causing drag and noise should be eliminated, and the structural complexity should be decreased. Nowadays, there is increasing interest in replacing this mechanical operating method with a comparatively light and simple morphing system (Cloyd, 1998; Thill *et al.*, 2008).

Shape memory alloys (SMAs) have attractive characteristics such as the shape memory effect and the superelasticity, because there are three phases in SMAs: martensite, austenite, and R-phase. The martensite changes to the austenite when the temperature increases, and the reverse occurs when the temperature decreases. M_s denotes the temperature at which the

austenite starts to change to the martensite, and M_f denotes the temperature at which the phase transformation is complete. A_s denotes the temperature at which the martensite starts to change to the austenite, and A_f denotes the temperature at which the phase transformation is complete. The R-phase may or may not exist, depending on the manufacturing process for the alloy. Under the phase-transformation temperature (A_f), the shape memory effect occurs when the temperature is raised. The residual strains are fully recovered, and the original shape is recovered at the phase-transformation temperature (A_f). Superelasticity occurs above the phase-transformation temperature (A_f). The alloy returns to its initial elastic state after being loaded and unloaded, and this process follows a hysteresis curve. These characteristics were first discovered in 1951, and the shape memory effect was observed in 1963. Since then, SMAs have become commercially available, and are used in many areas (Otsuka and Wayman, 1998). Copper alloys and NiTi series (Nitinol) SMAs are commonly used alloys that exhibit the shape memory effect (Duerig *et al.*, 1999). Nitinol SMAs provide a great deal of energy per unit volume, excellent corrosion resistance and biocompatibility, and long service lives, more than 100 000 cycles. Therefore, SMAs could be used for excellent actuators (Lee *et al.*, 1999).

The SMA wire actuator was developed to control the shape of a morphing wing in this research. A change in the camber of a morphing wing has the same effect as the operation of a mechanical flap, while reducing the drag caused by the discontinuous parts of the flap so that the aerodynamic characteristics can be significantly improved. Although the response of the SMA wire actuator is slow, it was selected for this purpose because a fast response is not required to operate a flap. Material property tests and actuation characteristic tests of the SMA wire actuator were carried out, and Flexinol wire was selected as the most suitable actuator. Developed actuators were used to operate a morphing flap, and actuation characteristic tests of the morphing wing were performed. Matlab/Simulink was used to design the system which is to investigate the response characteristics by measuring the displacement of the structures deformed by the commanded current. The morphing wing was smoothly deformed when the commanded current was supplied.

2. Experiments of the SMA wire actuator

2.1. DSC tests

Even the material properties of SMAs are already known, their precise values must be determined since these alloys exhibit complex nonlinear behavior, and their characteristics can be altered easily by the manufacturing variables. Two types of Nitinol SMA wire were considered as actuators for the morphing wing: SM495 (NDC) and Flexinol (Dynalloy, Inc.), which have different compositions. Characteristic tests were conducted for each type to assess its suitability as an actuator. Table 1 lists the properties of each SMA and Table 2 lists diameters and phase-transformation temperatures (A_f) of the wires, obtained from the product data sheet.

Differential scanning calorimeter (DSC) tests were carried out for two types of SMA wires (SM495 and Flexinol) to determine phase-transformation temperatures (A_s , A_f). These tests were only conducted for SM495 #1 and Flexinol #2 since different diameters of the same wire had the same composition. Figure 1 shows results of these tests.

The SMA actuator is operated by changing its temperature, and the force is usually generated when the martensite phase changes to the austenite phase. The measured phase-transformation temperature A_f was 67°C for SM495, and 80°C for Flexinol. These results differ slightly from values of Table 2. The phase-transformation temperature of an SMA is related to its stress state, and tends to increase with increasing applied stress. The R-phase appeared in all specimens during DSC tests; this phase can vary according to the heat-treatment (annealing) temperature. An SMA whose phase-transformation temperature exceeds room temperature will exhibit a

Table 1. Basic material properties of SMAs

SM495 (NDC)	Flexinol (Dynalloy, Inc.)
– Nickel: 54.5 wt%	– Thermal conductivity: 0.18 W/cm°C
– Titanium: balance	– Specific heat: 0.2 cal/g°C
– Oxygen: max. 0.05 wt%	– Latent heat of transformation: 5.78 cal/g
– Carbon: max. 0.02 wt%	– Melting point: 1300°C
– Melting point: 1310°C	– Density: 6.45 g/cm ³
– Density: 6.5 g/cm ³	– Electrical resistivity
– Electrical resistivity: 76 μ Ohm cm	– Martensite: 80 μ Ohm cm
– Modulus of elasticity: 28-41 $\cdot 10^3$ MPa	– Austenite: 100 μ Ohm cm
– Thermal expansion coefficient: 6.6 $\cdot 10^{-6}$ /°C	– Thermal expansion coefficient
– Ultimate tensile strength: 1100 MPa	– Martensite: 6.6 $\cdot 10^{-6}$ /°C
– Total elongation: 10%	– Austenite: 11.0 $\cdot 10^{-6}$ /°C

Table 2. Types of SMA wire

SMA wire	Diameter [mm]	A_f temperature [°C]
SM495 #1	0.20	~ 75
SM495 #2	0.50	~ 75
Flexinol #1	0.15	70
Flexinol #2	0.20	70
Flexinol #3	0.38	70
Flexinol #4	0.51	70

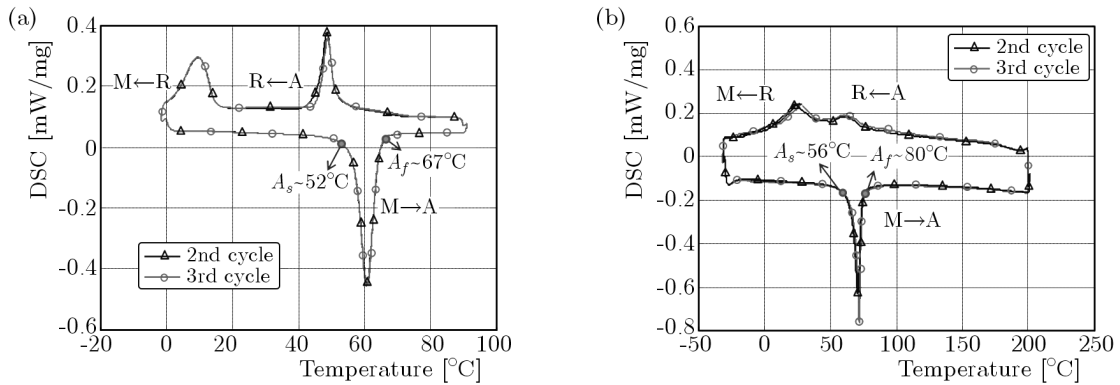


Fig. 1. Results of DSC tests: (a) SM495 #1, (b) Flexinol #2

shape memory effect at room temperature, and can be used as an actuator. Therefore, SM495 and Flexinol are both appropriate for use as actuators.

2.2. Actuation characteristic tests

The temperature of a SMA wire varies when it is used as an actuator. Typically, the temperature is increased by electric heating and decreased by natural cooling, such as convection and radiation. When a SMA wire is heated electrically, it is important to determine the appropriate voltage or current to maintain the temperature within the operational range. Electric heating raises the temperature very quickly, and this sometimes leads to over-current. Over-current causes the heat treatment (annealing) of a SMA wire actuator and the material properties change. As a result, the characteristics of the actuator also change. Accordingly, several experiments were carried out to measure the appropriate operational current for the SMA wire actuator.

2.2.1. Testing procedure

The length of each SMA wire was 10 cm, and its ends were fixed (Fig. 2). The force was measured by a load cell at one end of the wire while a constant current was supplied to the wire. A square-wave current was applied three times, and was increased in 0.1 A increments from 0.3 A to 1.2 A in order to determine the appropriate current.

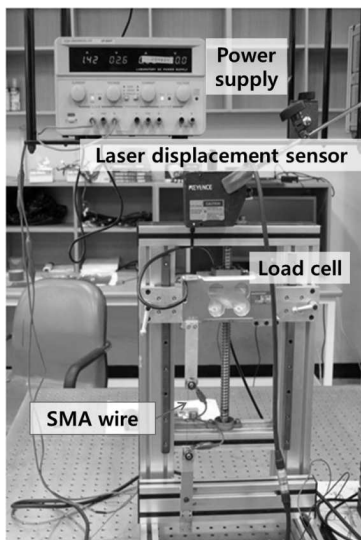


Fig. 2. Experimental setup

2.3. SM495 wire

The force generated by SM495 wire varies according to the initial strain (pre-strain). Therefore, experiments were performed under different initial conditions (1%, 2%, 3%, and 4% of pre-strain) to investigate the characteristics in terms of pre-strain. Figure 3 shows results obtained by measuring the force under each pre-strain condition as the current was increased gradually. The generated force increased with increasing pre-strain, and also with the increasing current up to about 0.6 A in all cases. The maximum force was generated at 0.6-0.7 A. Above 0.8 A, large force variations began to appear, and the force decreased as the current increased. At low currents, the temperature increase was inadequate, and the force generated by shrinkage caused by the shape memory effect of the SMA wire was low. On the other hand, at over-currents, the temperature increase was excessive, the properties of the wire were changed, and the force was diminished again. Therefore, an applied current under 0.5 A did not raise the temperature of the wire sufficiently to generate the maximum force. At currents over 0.8 A, the temperature increase was excessive and properties of the wire were altered, resulting in material degradation. Based on these results, 0.6 A was considered the appropriate current for the SM495 #1 (diameter: 0.2 mm) specimen.

Table 3. Response characteristics of the SM495 #1 wire actuator

SM495 wire	Frequency [Hz]	Max. force [N]	Power for 10 cm length
1% pre-strain	0.2	15	1.26 W
2% pre-strain	0.17	19	1.26 W
3% pre-strain	0.13	21	1.26 W
4% pre-strain	0.12	22	1.26 W

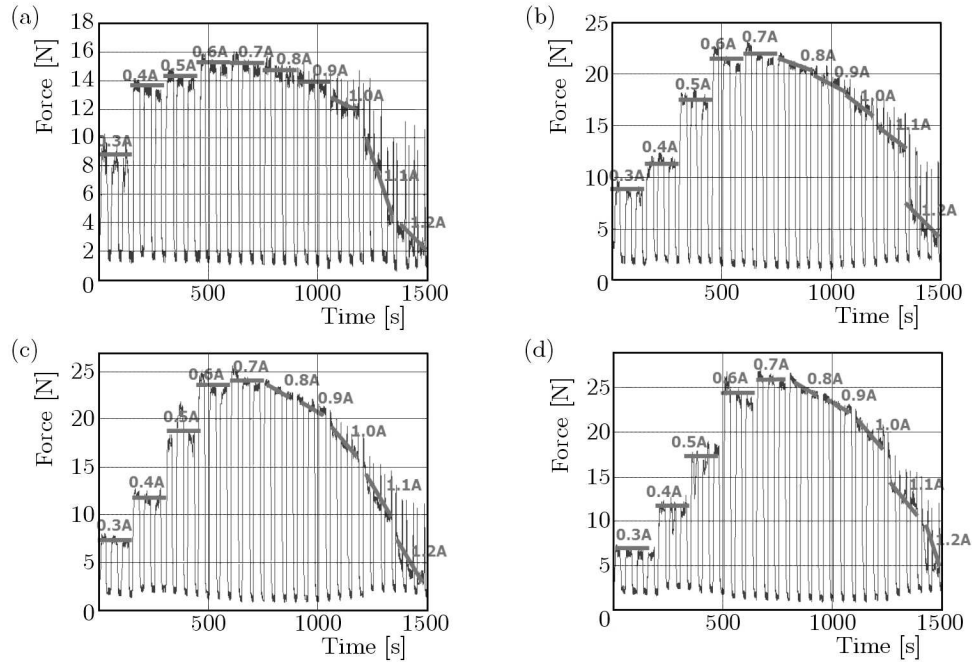


Fig. 3. Generated force by SM495 #1 (diameter: 0.2 mm) according to the current; (a) 1% pre-strain, (b) 2% pre-strain, (c) 3% pre-strain, (d) 4% pre-strain

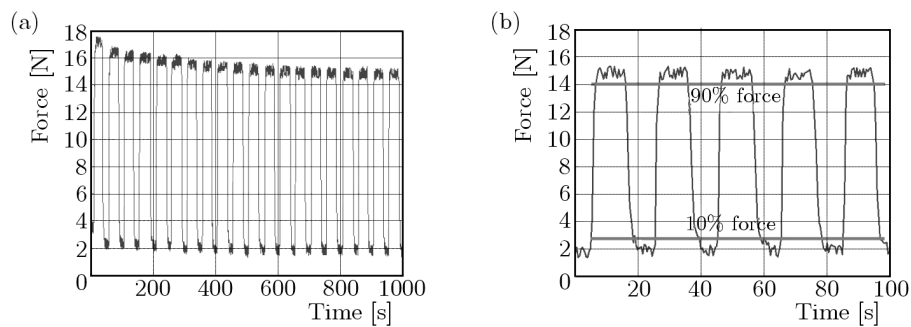


Fig. 4. (a) Generated force by SM495 #1 at 0.6 A. (b) Response time of SM495 #1

As shown in Fig. 3, the generated force gradually decreased when a 0.6 A current was applied three times. The reason for this was due to phase reorientation that occurred to stabilize the internal stress when the current started to flow. The 0.6 A current was applied repeatedly until the force converged. Figure 4a shows the force under repeated applications of the current in the 1% pre-strain case. The force generated by the wire gradually decreased as the number of applications of the current increased, and converged after 20 cycles in all cases. The response time according to the square wave current was measured when the force converged. Specifically, the response time was investigated by the sum of two periods; the time until the force reached 90% of its maximum when the current was supplied, and the time until the force decreased to 10% of its maximum when the current was cut off (Fig. 4b). Table 3 lists the response frequencies, maximum forces, and required power for the 10-cm SM495 #1 wire specimen according to the pre-strain.

2.3.1. Flexinol wire

Variation of the generated force according to the pre-strain was not observed for the Flexinol wire (Fig. 5). Therefore, the response characteristics of Flexinol were investigated in the absence of the pre-strain; the results are presented in Table 4 and Fig. 6.

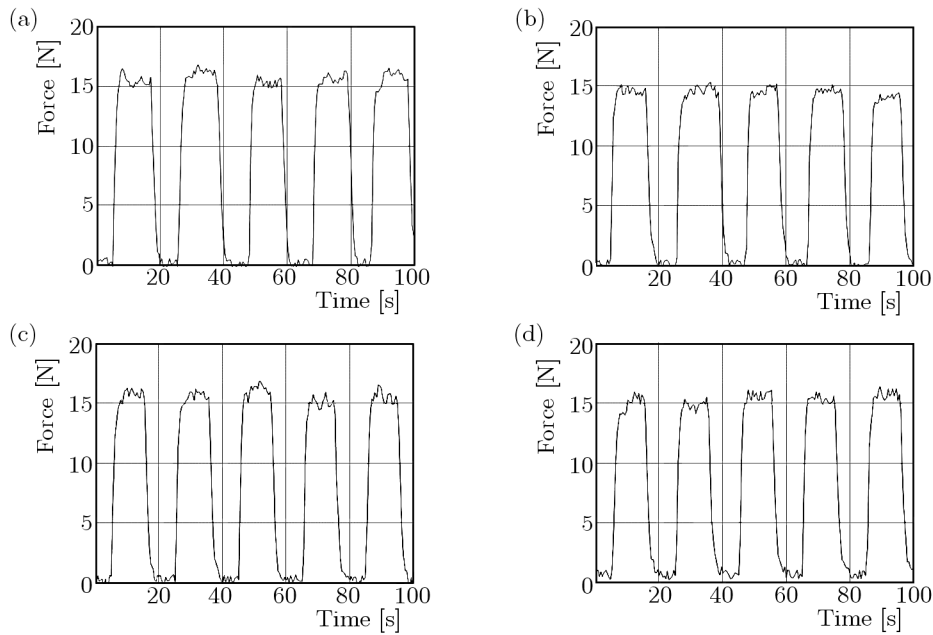


Fig. 5. Generated force by Flexinol #1 (diameter: 0.15 mm) according to the pre-strain at 0.5 A; (a) 1% pre-strain, (b) 2% pre-strain, (c) 3% pre-strain, (d) 4% pre-strain

Table 4. Response characteristics of Flexinol

Flexinol wire	Current [A]	Max. force [N]	Frequency [Hz]	Power for 10 cm length
Flexinol #1	0.5	15	0.20	1.55 W
Flexinol #2	0.7	25	0.18	1.47 W
Flexinol #3	1.7	95	0.07	3.91 W
Flexinol #4	2.4	145	0.04	3.80 W

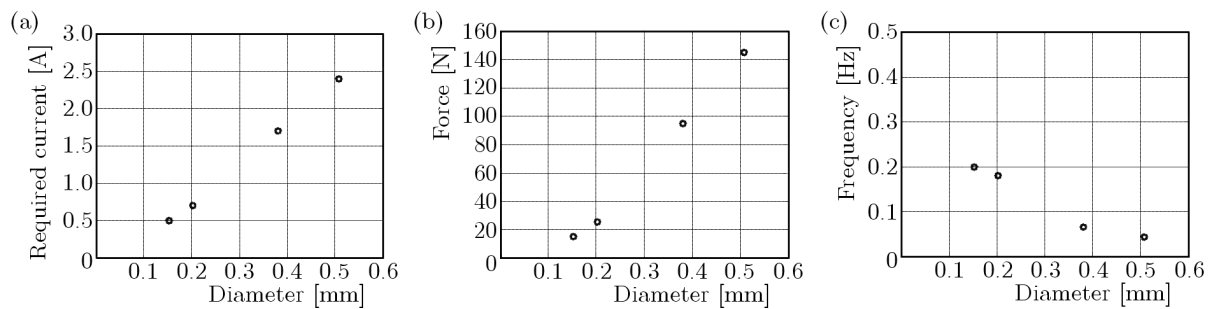


Fig. 6. Results of actuation characteristic tests of Flexinol; (a) appropriate current, (b) maximum force, (c) response frequency

The appropriate current and maximum force for Flexinol increased quadratically with respect to the diameter. The reason for this was the constant stress-strain relationship for the given material, so that the cross-sectional area of the wire was proportional to the required current and the force. The response frequency was inversely proportional to the wire diameter. The volume per unit length increased quadratically with respect to the wire diameter, and thus heating and cooling required more time because of the increased heat capacity.

As a linear actuator, the Flexinol wire is more advantageous than the SM495 wire because the generated force does not vary appreciably according to the pre-strain.

2.4. Stress-strain tests of Flexinol wires

Since the deformation of an SMA wire varies according to the applied force, it is necessary to determine the appropriate operational range of forces for each type of the wire in order to design an actuator. Therefore, stress measurement experiments were performed for the four types of Flexinol wires. A constant force was applied to the Flexinol wire, and the displacement of the end of the wire was measured to determine the deformation under periodic application of the current listed in Table 4. Weights were suspended from the end of the wire to apply the constant force (Fig. 7). A laser displacement sensor was used to measure the displacement of the end of the wire. The displacements obtained when the constant force was applied to the Flexinol #1 wire are shown in Table 5. The initial length of the wire was 300 mm. The wire contracted when it was heated by the applied current, and was stretched by the suspended weights when it cooled while the current was cut off. However, the amount of extension during cooling gradually decreased when the force applied by the suspended weights was insufficient (0.27 N, 0.54 N, and 1.03 N). These results show that if the force applied to the wire is inadequate, the wire cannot be recovered to its initial shape after deformation. When the applied force was appropriate (2.02 N, 2.98 N, and 3.94 N), the amount of the deformation was constant, and the wire was fully recovered to its initial length when the current was repeatedly supplied and cut off. On the other hand, when the excessive force was applied (6.87 N, 7.85 N, and 9.81 N), the wire was stretched beyond its initial length as the current was repeatedly applied. In the 6.87 N and 7.85 N cases, the amount of extension during cooling converged as the number of current cycles increased. This means that the characteristics of the SMA wire actuator change when the excessive force is applied, but the behavior of the actuator is stabilized after repetitive operation. When 9.81 N was applied, the length of the wire increased with the number of current cycles, and the wire was finally broken.

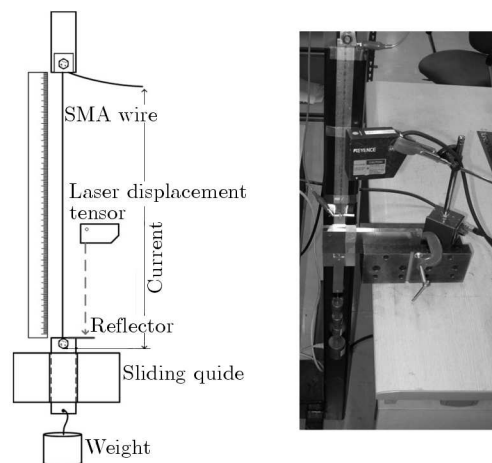
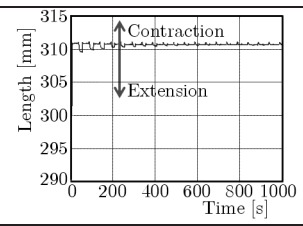
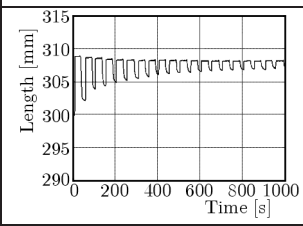
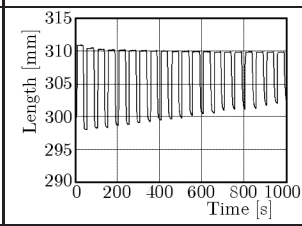
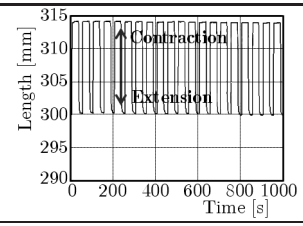
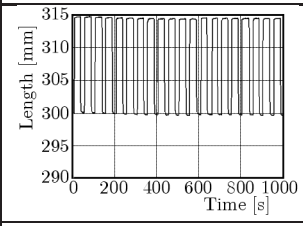
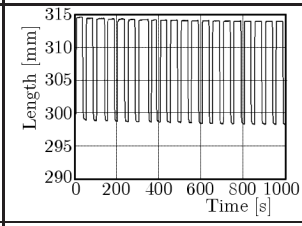
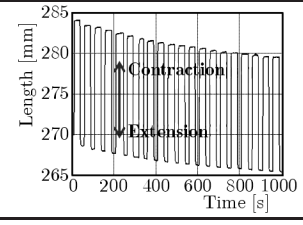
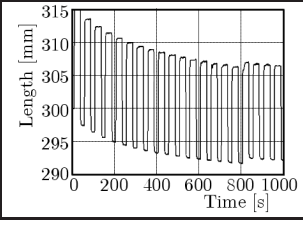
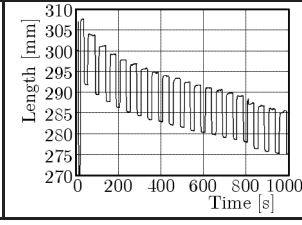


Fig. 7. Experimental setup for measuring the strain on a Flexinol wire

Figure 8a shows the strain of the Flexinol #1 wire according to the applied force for the applied currents of 0.3, 0.4, and 0.5 A. The strain of the wire decreased at the currents lower than the appropriate current, and was about 5% at the appropriate current of 0.5 A when a 3–7 N force was applied. From these results, the appropriate range of the applied force per wire was 3–5 N when the actuator was designed using the Flexinol #1 wire. Figure 8b shows the strain according to the applied stress for the four types of Flexinol wires; all of them exhibited similar tendencies. The measured appropriate stress range for effective operation was 200–500 MPa.

Table 5. Deformation of the SMA Flexinol #1 wire according to the applied force

Force	0.27 N	0.54 N	1.03 N
Displacement of the end of the wire			
Force	2.02 N	2.98 N	3.94 N
Displacement of the end of the wire			
Force	6.87 N	7.85 N	9.81 N
Displacement of the end of the wire			

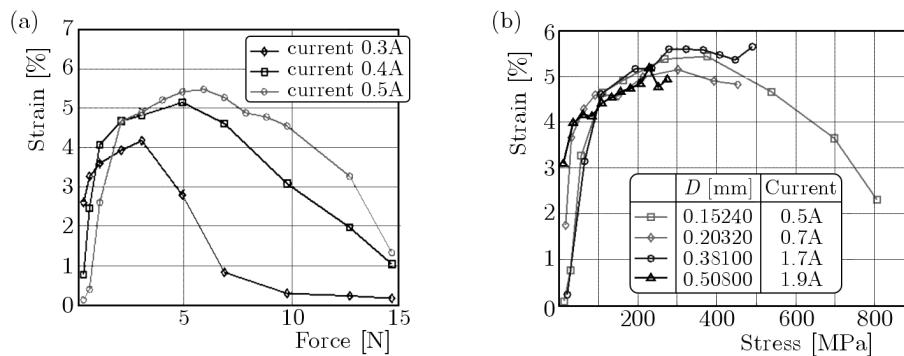


Fig. 8. Strain on the Flexinol #1 wire (a) and strain for the four types of Flexinol wires (b)

2.5. Response of Flexinol wire actuators to a commanded input current

The system used to investigate the response characteristics of the SMA wire actuator was designed via Matlab/Simulink. This system measured the displacement response to a commanded input current. The Flexinol wire with a diameter of 0.20 mm (Flexinol #2) was selected as the most suitable actuator among the four types of Flexinol wires since its response was relatively fast and it generated a large force. A constant force was applied by suspending a mass of 650 g from the end of the actuator. The commanded input current was supplied to the actuator by the designed control algorithm system. An additional current amplifier was included in this system because the output current of the data acquisition (DAQ) board was insufficient to operate the actuator. The amplified current operated the actuator, and the length of the actuator changed accordingly. The laser displacement sensor measured the displacement of the end of the actuator to determine the change in the length of the actuator. The DAQ board collected data, and they were stored in the personal computer (PC) memory (Fig. 9).

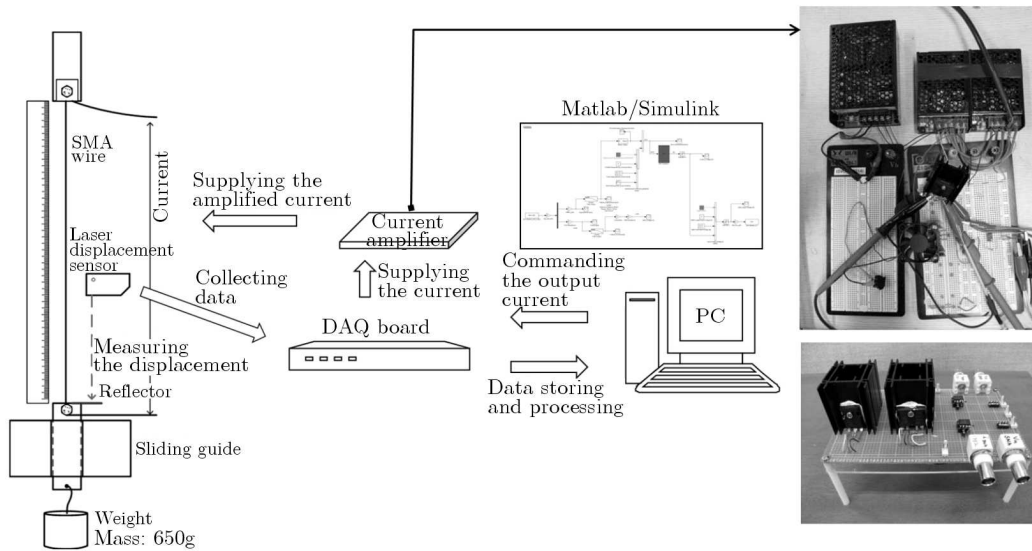


Fig. 9. System to measure the displacement response to a commanded input current

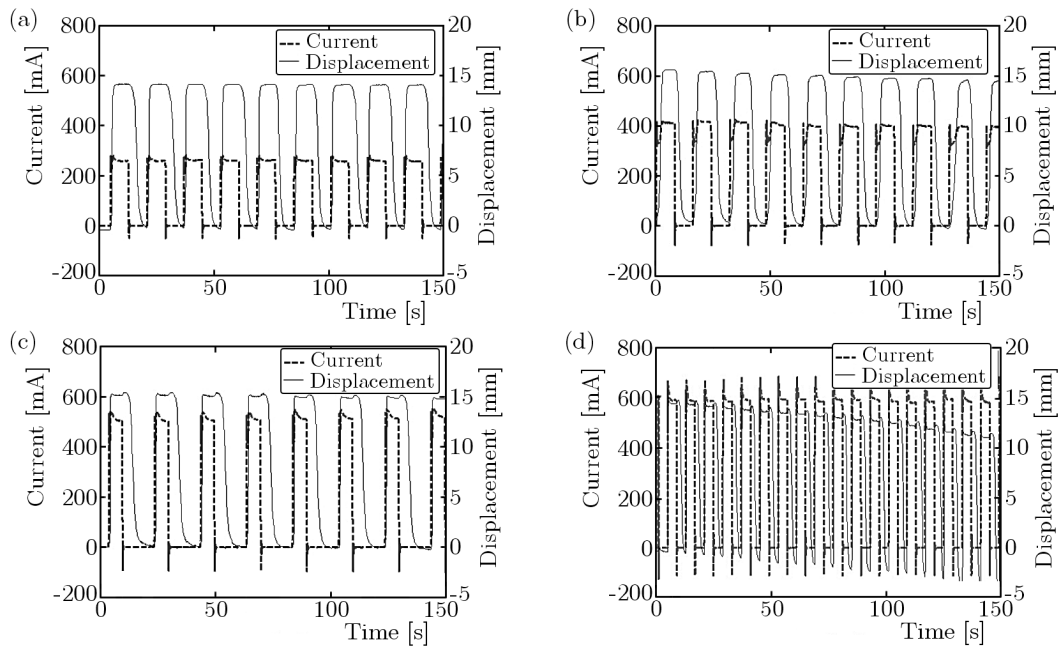


Fig. 10. Deformation of the SMA wire actuator according to the square wave input current; length change at: (a) 300 mA, (b) 400 mA, (c) 500 mA, (d) 600 mA

The experiments were performed for four different commanded currents: square wave currents of 300, 400, 500, and 600 mA. In these tests, it took more time when the commanded current was cut off than when the commanded current was applied. The output displacement was relatively constant in response to the 300, 400, and 500 mA command input currents (Fig. 10). As noted in Section 2.2.3, if the current supplied to the SMA wire actuator is more than 700–800 mA, the material properties are degraded, and the length of the SMA wire is gradually extended as the number of current cycles increases. When the input current was 600 mA, the length of the SMA wire actuator was extended (Fig. 10d). The one possible reason for this phenomenon could be concerned as that the additional current amplifier operated as an independent system when the commanded current was applied and it caused an overshoot. This overshoot may have caused the current to exceed 700 mA so that the properties of the SMA were degraded. Therefore, a control

algorithm to cut the current when it exceeds the critical current level should be developed and added to the system.

The output displacement was measured under an increasing step commanded current (0 mA \rightarrow 100 mA \rightarrow 200 mA \rightarrow 300 mA \rightarrow 400 mA \rightarrow 500 mA \rightarrow 400 mA \rightarrow 300 mA \rightarrow 200 mA \rightarrow 100 mA \rightarrow 0 mA) (Fig. 11). It was not proportional to the input current due to the nonlinearity of the material properties of the SMA. This output displacement jumped sharply at the 300 mA step when the current was increasing, and dropped sharply at the 100 mA step when the current was decreasing. The cause of this phenomenon was attributed to SMA phase transformation, which indicates that hysteretic behavior occurred when the current was applied.

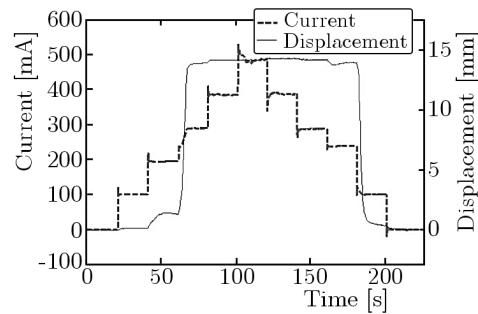


Fig. 11. Deformation of the SMA wire actuator according to the increasing/decreasing input current

3. Experiments on the morphing wing

3.1. Actuation characteristic tests of the morphing wing

Conventional mechanical hinges, such as those that connect the flaps to the main wings, cause aerodynamic loss. This problem can be improved by using a morphing wing that provides the same functionality without hinges. The morphing wing model developed by Kang *et al.* (2012) was used in this research. The current was supplied to the SMA wire actuator installed in the morphing wing model to operate it, and the flap rotated smoothly. The applied current was increased to investigate the relationship between the current and the flap angle. The angular displacement of the flap increased linearly in the range 1.5-2.7 A, but exhibited nonlinear behavior when the current exceeded 2.7 A. The reason for this appears to be that excessive applied current caused heat-treatment, and the properties of the SMA wire were degraded.

According to the results of an aerodynamic analysis of the morphing wing at a flight velocity 20 m/s, the difference between the pressure coefficients of the upper and lower skins increased as the flap angle increased from 0° to 6.4° to 15.9°. The highest lift-to-drag ratio was estimated at 15.22 when the flap angle was 6.4°; this was because both the lift and drag coefficients increased when the flap angle increased (Kang *et al.*, 2012). This means, it is necessary to determine the most efficient flap angle to improve the aerodynamic efficiency, instead of simply increasing the flap angle unconditionally.

3.2. Response to a commanded input current

The system used to investigate the response characteristics of the morphing wing was designed via Matlab/Simulink. This system was used to measure the displacement response to a commanded input current. The Flexinol wire with a diameter of 0.20 mm (Flexinol #2) was used as the actuator of the morphing wing. The input current (controlled by the PC) was supplied by the DAQ board and amplified by the current amplifier to operate the morphing wing (Fig. 12). To verify the deformation, the displacement of the trailing edge of the flap was measured instead of the flap rotation angle.

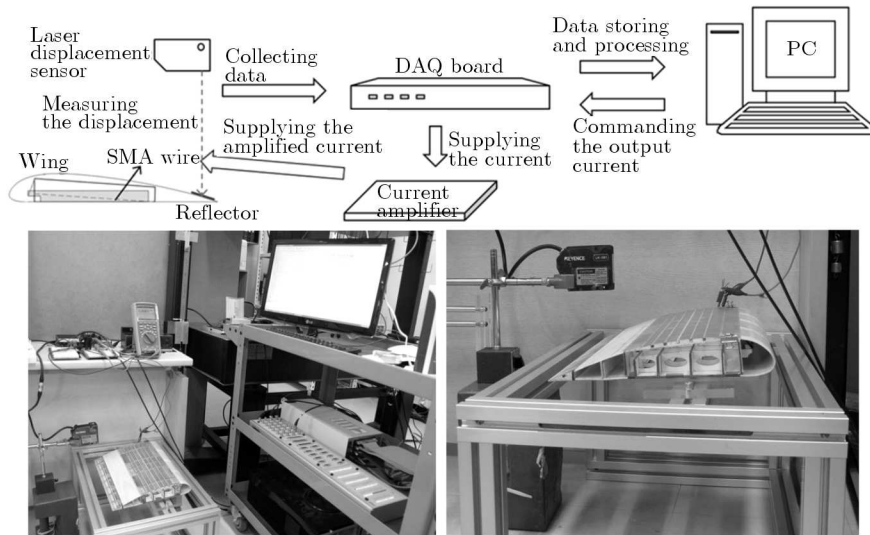


Fig. 12. System to measure the displacement response to a commanded input current

The time required for the displacement to reach 80% of the converged value was recorded as the response time. The response time was 10.34 s when a constant current of 2 A was applied, and 3.8 s when the current was cut off. The response was faster when the current was cut off than when the current was applied, which is contrary to the results obtained for the SMA wire. The reason can be considered as that the elastic force of the morphing wing and the additional rubber ring shortened the response time when the current was cut off. When the increasing/decreasing step input current (0 mA \rightarrow 500 mA \rightarrow 1000 mA \rightarrow 1500 mA \rightarrow 2000 mA \rightarrow 1500 mA \rightarrow 1000 mA \rightarrow 500 mA \rightarrow 0 mA) was applied, large variations of the displacement occurred at 1000, 1500, and 2000 mA. The nonlinear behavior of the SMA wire during the phase transformation could be the reason for this phenomenon (Fig. 13).

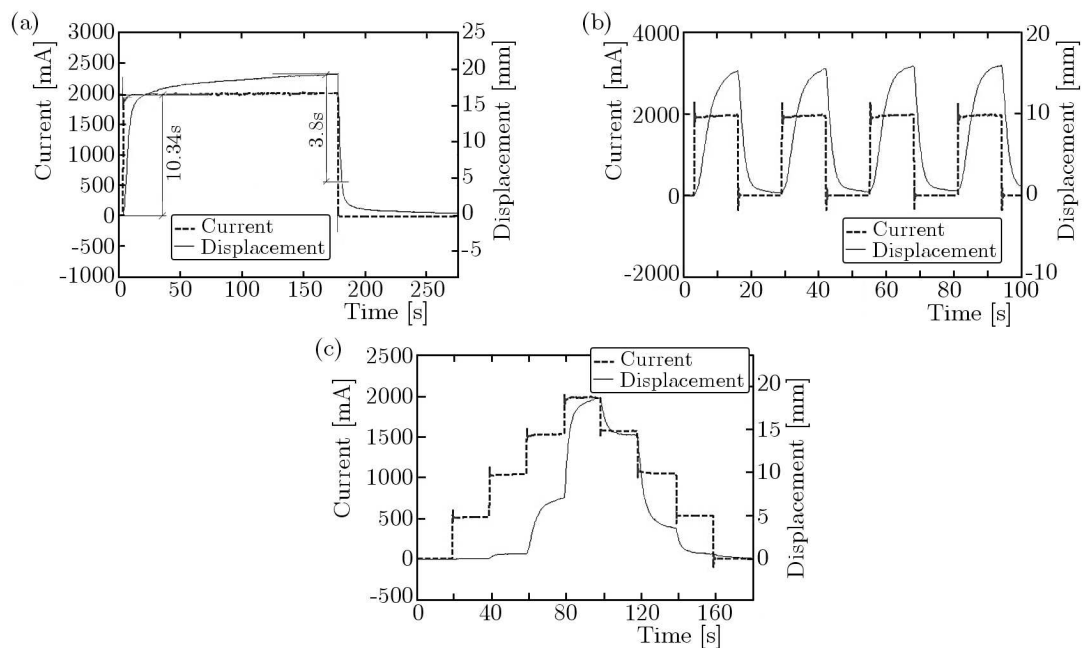


Fig. 13. Displacement of the trailing edge of the morphing wing; (a) constant current of 2 A, (b) square wave current of 2 A, (c) increasing/decreasing current

4. Conclusion

The characteristics of the SMA wire actuator and the morphing wing operated by this actuator were investigated in this research. DSC tests were carried out to confirm the exact material properties of SMAs, such as the phase-transformation temperature. SM495 and Flexinol both exhibited the shape memory effect at room temperature, and hence both were deemed suitable for use as actuators. Several actuation characteristic tests were performed on the SMA wire actuators, and the appropriate currents were measured. For the SM495 wire with a diameter of 0.2 mm (SM495 #1), the generated force increased with the pre-strain. A current less than 0.5 A was insufficient to fully heat this wire, and a current over 0.8 A was excessive, causing degradation of the SMA properties. Consequently, 0.6-0.7 A was considered appropriate for operating this SMA wire actuator. For Flexinol, on the other hand, significant variation of the generated force according to the pre-strain was not observed, and thus the response characteristics were investigated without the pre-strain. The appropriate current and the maximum generated force increased quadratically with respect to the diameter. Flexinol was selected as a more suitable actuator because it was less affected by the pre-strain than SM495. Since the deformation of an SMA varies according to the applied force, it was necessary to investigate the appropriate range of applied forces. Therefore, stress-strain tests were conducted for the four types of Flexinol wires with different diameters considered in this study. When a current lower than the appropriate current was supplied to the wire, the strain decreased. The maximum strain of 5% appeared when 200-500 MPa of stress was applied to the wire at the appropriate current. This stress range was considered to be the appropriate range; all four types of Flexinol wires exhibited similar tendencies. Based on the results of these experiments, Flexinol #2, which had a diameter of 0.2 mm, was selected as the actuator to operate the morphing wing. The system was designed via Matlab/Simulink to investigate the response characteristics of the SMA wire actuator and morphing wing structures to the commanded input current. The SMA wire actuator and the morphing wing deformed smoothly, but also exhibited nonlinear behavior due to the phase transformation of the SMA at certain current levels. This phenomenon should be considered when the SMA wire actuator is designed for use in structures such as morphing wings.

Acknowledgements

This research was supported by the KARI-University Partnership Program. This research was also partly supported by WCU (World Class University) program through the National Research Foundation of Korea funded by the Ministry of Education, Science and Technology (R31-2008-000-10045-0).

References

1. BOWMAN J., SANDERS B., CANNON B., KUDVA J., JOSHI S., WEISSHAAR T., 2007, Development of next generation morphing aircraft structures, *Proc. 48th AIAA/ASME/ASCE/AHS/ASC Structures, Structural Dynamics and Materials Conf. (SDM)*, AIAA-2007-1730
2. CLOYD J.S., 1998, Status of the United States Air Force's more electric aircraft initiative, *IEEE Aerospace and Electronic Systems Magazine*, **13**, 4, 17-22
3. DIACONU C.G., WEAVER P.M., MATTIONI F., 2008, Concepts for morphing airfoil sections using bi-stable laminated composite structures, *Thin-Walled Structures*, **46**, 6, 689-701
4. DUERIG T., PELTON A., STOCKEL D., 1999, An overview of nitinol medical applications, *Materials Science and Engineering, A*, **273/275**, 149-160
5. JOSHI S.P., TIDWELL Z., CROSSLEY W.A., RAMAKRISHNAN S., 2004, Comparison of morphing wing strategies based upon aircraft performance impacts, *Proc. 45th AIAA/ASME/ASCE/AHS/ASC Structures, Structural Dynamics and Materials Conf. (SDM)*, AIAA-2004-1722

6. KANG W.R., KIM E.H., JEONG M.S., LEE I., 2012, Morphing wing mechanism using a SMA wire actuator, *International Journal of Agricultural and Soil Science*, **13**, 1, 58-63
7. LEE H.J., LEE J.J., HUH J.S., 1999, A simulation study on the thermal buckling behavior of laminated composite shells with embedded shape memory alloy (SMA) Wires, *Composite Structures*, **47**, 1/4, 463-469
8. MATTIONI F., GATTO A., WEAVER P.M., FRISWELL M.I., POTTER K.D., 2006, The application of residual stress tailoring of snap-through composites for variable sweep wings, *Proc. 47th AIAA/ASME/ASCE/AHS/ASC Structures, Structural Dynamics, and Materials Conf. (SDM)*, AIAA-2006-1972
9. OTSUKA K., WAYMAN C.M., 1998, *Shape Memory Materials*, Cambridge University Press
10. SANDERS B., ESTEP F.E., FORSTER E., 2003, Aerodynamic and aeroelastic characteristics of wings with conformal control surfaces for morphing aircraft, *Journal of Aircraft*, **40**, 1, 94-99
11. SANDERS B., REICH G.W., JOO J.J., 2005, Conceptual skin design for morphing aircraft, *Proc. 16th Int. Conf. on Adaptive Structures and Technologies (ICAST)*, **16**, 275-281
12. THILL C., ETCHES J., BOND I., POTTER K., WEAVER P., 2008, Morphing skins, *Aeronautical Journal*, **112**, 1129, 117-139

Manuscript received August 8, 2013; accepted for print December 1, 2013